Bioorganic Chemistry 41-42 (2012) 6–12

Contents lists available at SciVerse ScienceDirect

Bioorganic Chemistry

journal homepage: www.elsevier.com/locate/bioorg

Chemical and biological evaluation of some new antipyrine derivatives with particular properties

C. Remes [a], A. Paun [a], I. Zarafu [a], M. Tudose [b], M.T. Caproiu [c], G. Ionita [b], C. Bleotu [d], L. Matei [d], P. Ionita [a,*]

[a] University of Bucharest, Department of Chemistry, Biochemistry and Catalysis, 90-92 Panduri, Bucharest 050663, Romania
[b] Institute of Physical Chemistry, 202 Spl. Independentei, Bucharest 060021, Romania
[c] Institute of Organic Chemistry, 202A Spl. Independentei, Bucharest 060023, Romania
[d] Institute of Virology, 285 M. Bravu, Bucharest 030304, Romania

ARTICLE INFO

Article history:
Received 2 December 2011
Available online 2 January 2012

Keywords:
Antipyrine
Crown ether
NBD
Nitroxide
Isoniazid
Synthesis

ABSTRACT

Starting from 4-amino-antipyrine, six new compounds were synthesized and characterized. The new compounds contain moieties with particular properties, such are ionophore (benzo-15-crown-5), fluorescent (nitrobenzofurazan), stable free radical (nitroxide), or other types of biological active residues, like nitroderivatives, antipyrine or isoniazid residues. They were fully characterized by appropriate means (^{1}H and ^{13}C NMR, IR, UV–Vis, fluorescence, EPR, elemental analysis) and some of their biological properties were evaluated. Hydrophobicity (R_{M0}, log *P*), total antioxidant capacity (*TAC*), and antimicrobial properties are also presented and discussed.

1. Introduction

Antipyrine or phenazone (1,2-dihydro-1,5-dimethyl-2-phenyl-3*H*-pyrazol-3-one) derivatives are well known compounds used mainly as analgesic and antipyretic drugs [1]. One of the best known antipyrine derivatives is 4-aminoantipyrine or 4-AAP (4-amino-2,3-dimethyl-1-phenyl-3-pyrazolin-5-one), which presents a structural similarity with metamizole, a well-known and very effective analgesic, anti-inflammatory and antipyretic agent [2].

Antipyrine is completely absorbed and uniformly distributed in the body in 1 h after oral ingestion [3,4], being thus proposed as a very suitable marker for measuring oxidative stress. The metabolic pathway of antipyrine has been extensively studied and showed that most of it is excreted in urine as 3- and 4-hydroxyantipyrine [5–7].

Protection against oxidative stress as well as prophylactic of some diseases including cancer is important directions in medicine and biochemistry [8,9]. Reactive oxygen species (ROS), including free radicals, led to a decrease in the antioxidant capacity, and, moreover, may generate other reactive species that damage the living cell. Oxidative stress may arise in a biological system after an increased exposure to oxidants, so the antioxidants play a major role in protecting biological systems against such threats. Different types of antioxidants (vitamins C and E, glutathione, lipoic acid, butylated phenols, etc.) have been widely used in different fields of industry and medicine as compounds that interrupt radical-chain oxidation processes, causing thus a high scientific interest [10,11].

Antipyrine derivatives are strong inhibitors of cycloxygenase isoenzymes, platelet tromboxane synthesis, and prostanoids synthesis [1,12]. The biological activity of these compounds has also been attributed to its scavenging activity against reactive oxygen and nitrogen species, as well as to the inhibition of neutrophil's oxidative burst. However, besides its well recognized benefits, antipyrine derivatives have been associated with potential adverse effects characterized by leukopenia, most commonly of neutrophils, causing neutropenia in the circulating blood (agranulocytosis). It is worth to mention that there are studies demonstrating that this adverse effect might be exaggerated [2,13]. Several congeners and transition metal complexes of antipyrine were also biological evaluated [14], being reported with antivirus and antibacterial activity [15,16].

In this work we present the synthesis and structural characterization of six new compounds derived from antipyrine, together with some of their biological evaluation data.

2. Results and discussion

2.1. Synthesis and structural characterization

The aim of our work focused on the synthesis and structural characterization of some novel antipyrine derivatives, with potential significant biological activity, starting from 4-AAP. Thus, 4-AAP

* Corresponding author. Fax: +40 213121147.
E-mail address: pionita@icf.ro (P. Ionita).

0045-2068/$ - see front matter © 2011 Elsevier Inc. All rights reserved.
doi:10.1016/j.bioorg.2011.12.003

was derivatized with different organic residues of organic, analytical or medicinal interest, such are benzo-15-crown-5 [17], the nitroxide stable free radical Tempo (2,2,6,6-tetramethylpiperidine-*N*-oxide) [18], isoniazid (an antibacterial drug used for the treatment of tuberculosis) [19], and nitrobenzofurazan (a fluorescent dye) [20]. In this way a number of six new compounds (Fig. 1) were obtained and appropriate characterized by different means (IR, UV–Vis, ^{1}H and ^{13}CNMR, fluorescence, EPR spectroscopy, etc.).

Compounds **1–6** were synthesized by simple coupling reactions, using the reactive amino group from the starting material, 4-AAP. The amino group acts as a nuclephile towards the other reagent used, leading finally to the desired compounds. The full practical procedures are presented under Experimental section.

To obtain compound **1**, first it was tried a direct synthesis using commercial available 4-carboxybenzo-15-crown-5 ether and involving N,N′-dicyclohexylcarbodiimide (DCC) as coupling agent; using this procedure, the yields in compound **1** was very poor (5%), so a new strategy was used, converting first the carboxyl group from 4-carboxybenzo-15-crown-5 ether into the corresponding acid chloride, much more reactive towards the nucleophilic amino group of 4-AAP. In this way compound **1** was obtained in satisfactory yields (50%). Compound **2** was obtained in a single reaction step, using 4-chloro-7-nitrobenzo-2-oxa-1,3-diazole (4-chloro-7-nitrobenzofurazan or NBD-chloride); two reaction systems were tried also, the first one using chloroform as solvent, with poor results (5%), and the second one using DMF as solvent, with better efficiency (20%). For compound **3**, it was necessarily to obtain first the acid chloride from 4-cloro-3,5-dinitrobenzoic acid, and further reaction of this with the 4-AAP afforded both compounds **3** and **4** (yields 80% and 20%, respectively). Compounds **5** and **6** are obtained from **3**, with good yields (80% and 60%, respectively), also in simple coupling reactions.

The chemical structure of the new compounds was confirmed by different spectral and elemental analysis. Thus, IR, UV–Vis, ^{1}H and ^{13}CNMR spectrometry was used for the compounds **1–4** and **6**; compound **5** is a stable free radical, and cannot be characterized by NMR, so EPR spectroscopy was employed [21]. The EPR spectrum consists mainly in the characteristic three lines of a nitroxide radical with a coupling constant of 15.40 G (Fig. 2a). Fluorescence was used to characterize compound **2** (due to the fluorescent NBD moiety); the maximum of the emission wavelength was 440 nm (Fig. 2b).

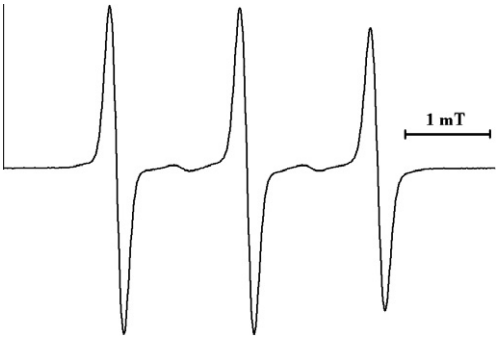

Fig. 2a. PR spectrum of **5**.

In order to elucidate some structural behavior of the new compounds, variable temperature NMR spectra have been used for a correct peaks attribution. An interesting case has been noticed for compound **6**. Due to the hindered free rotation induced by the two amide groups, the hydrogen atoms H-10 and H-14 are anizocrons; at room temperature the NMR signals are close to coalescence and are noticed only by the value of the integral; rising the temperature led to a single mediated peak in which the hydrogen atoms H-10 and H-14 are izocrons. For H-24 and H-25 it is noticed at $T = 303$ K the slow motion of the molecule, so a broad signal is noticed, and, moreover, the coupling between H-23 and H-26 is not evidenced. However, in GCOSY spectra the relationship between H-23 and H-26 with H-24 and H-25 is confirmed by the off-diagonal peak.

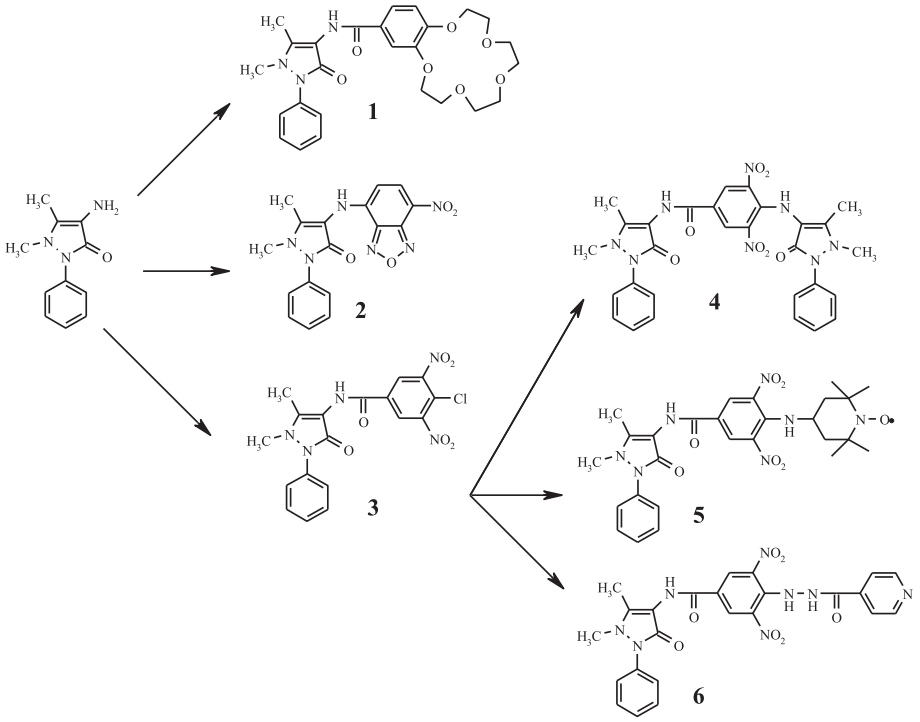

Fig. 1. Synthesis of the compounds **1–6**.

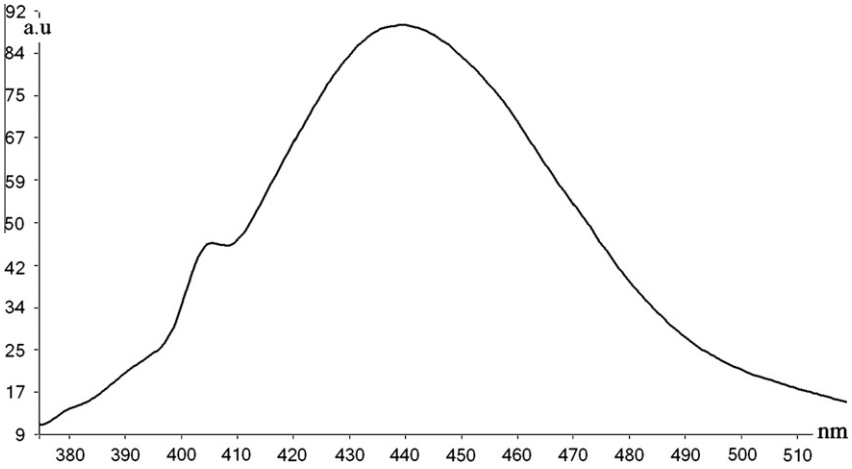

Fig. 2b. Fluorescence spectrum of **2**.

Table 1
Some physical data of the compounds **1–6**.

Comp.	λ_{max} (nm)[a]	R_f [b]	R_{M0}[c]	b[c]	TAC[d]	Log P[e]	PSA[e]
4-AAP	251, 281 (sh)	0.17	0.812	−1.581	92.65	0.809	52.962
1	261, 288 (sh)	0.08	1.471	−1.781	12.35	1.112	102.207
2	269, 324	0.46	1.280	−2.360	46.3	3.142	123.714
3	277	0.73	1.883	−1.183	22.2	2.668	147.685
4	278	0.09	2.091	−4.172	74.4	3.370	186.651
5	280	0.75	2.585	−1.993	17.35	4.236	183.178
6	271, 358	0.02	1.438	−4.129	63.35	1.351	201.702

[a] In methanol.
[b] Silica gel/ethyl acetate system.
[c] Determined lipophilicity and hydrophobic surface area.
[d] Total antioxidant capacity measured by DPPH method.
[e] Calculated hydrophobicity and polar surface area.

The purity of the compounds was checked by TLC. TLC can be used also for separation in preparative purposes. In our experiments the best system for separate simultaneously all the compounds **1–6** and the starting material 4-AAP was the chromatographic system made from analytical TLC plates (silica gel) and ethyl acetate as eluent. The R_f values thus obtained are compiled in Table 1. The most polar compounds are **1**, **4** and **6**. Table 1 compiles also the UV–Vis absorption data of all the compounds involved in this study.

2.2. Biological evaluation

2.2.1. Hydrophobicity (lipophilicity) and related measurements

The correlation between structure and compounds activity play an important role in the study of some biological interaction. Among the molecular properties the lipophilicity is important because the biological activity is correlated in QSAR studies (QSAR – Quantitative Structure Activity Relationships) with their capacity to cross the lipophil cell membrane. Lipophilicity influences the bioavailability and the drug absorption, drug–receptor interactions, metabolism of molecules, as well as their toxicity [22].

For a biological evaluation, it is important for the beginning to know the lipophilicity (or hydrophobicity) of the compounds; this step may be achieved by experimental measurements or just by using a computer predictor. Besides the classical methods of lipophilicity determination by the partition method of the compound between an immiscible polar and a non-polar solvent pair (usually *n*-octanol–water) [23], reversed phase thin layer chromatography (RP-TLC) is often used for evaluation of the organic – water partitioning properties of solutes owing to the simplicity and the rapidity of this method [24]. Thus, RP-TLC uses a non-polar stationary phase (such are silica gel impregnated with paraffin oil, silanized silica-gel, and C18 derivatized silica gel) and a mixture of two solvents, in which one is water (i.e. alcohol–water, acetone–water, acetonitrile–water, etc.). RP-TLC is widely used to measure the experimental lipophilicity (R_{M0}) and specific hydrophobic surface (b) using Eqs. (1) and (2). These values R_{M0} and b obtained as Eqs. (1) and (2) shows are the best indicators of the lipophilicity and the specific hydrophobic surface area of the compounds.

In our measurements we used analytical silica gel plates impregnated with paraffin oil, and as eluent a mixture of acetone with water in different proportions (50–90% acetone). The method starts with the measurement of the R_f values (see also Eqs. (1) and (2)) using different mixtures of acetone with water. The R_M values necessary for the determination of the hydrophobicity (lipophilicity) of the compounds is obtained as Eq. (1) shows. To measure the specific hydrophobic surface area b the linear correlation between the R_M values of our compounds and the concentration of organic solvent (C) in the eluent were calculated. The intercept R_{M0} is the R_M value of a compound extrapolated to zero organic phase concentration in the eluent and the slope b is the change of lipophilicity caused by unit concentration change of the organic phase.

A good linear correlation was found between R_M and C, characterized by high values of the correlation coefficient R (0.87–0.98) and good standard deviation values SD (0.06–0.37).

$$R_M = \log\left(\frac{1}{R_F} - 1\right) \quad (1)$$

$$R_M = R_{M_0} + bC \quad (2)$$

We can notice that the lowest R_{M0} values have been recorded in the case of 4-AAP and compound **6** (the isoniazid derivative). The highest values for R_{M0} have been recorded in the case of compound **5**.

The values obtained using the experimental RP-TLC method were correlated with the theoretically calculated hydrophobicity (log P) and molecular polar surface area (PSA) (Table 1) [25]. Good correlation of the measured R_{M0} values with the calculated log P (Table 1) is obtained, as shown in Fig. 3. The correlation coefficient R was 0.91 and the standard deviation SD was 0.37.

2.2.2. Total antioxidant capacity

It was mentioned before that antipyrine derivatives are active compounds against reactive oxygen and nitrogen species (ROS and RNS), and, moreover, the metabolic pathway of those compounds

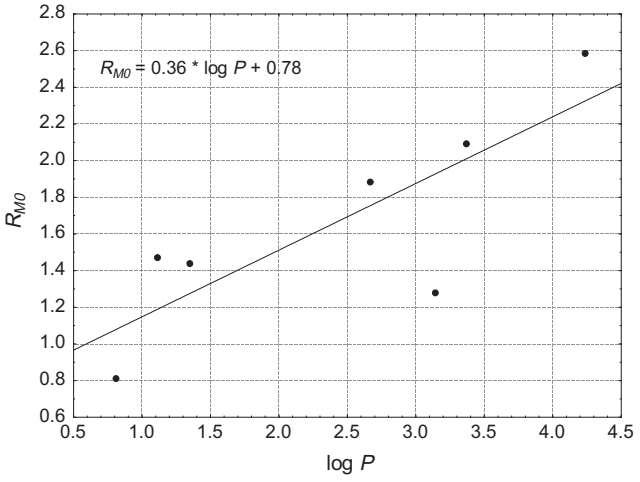

Fig. 3. Correlation of the measured R_{M0} values with the calculated log *P*.

involves the formation of the hydroxyl derivatives, the same type of compounds formed as well in reaction with ROS.

Among biological properties the total antioxidant capacity (*TAC*) represents one of the most used (also known as total antioxidant activity). There are different methods to measure *TAC*, and one of the best known involves the deep colored organic stable free radical, 2,2-diphenyl-1-picrylhydrazyl (DPPH); this method is also widely known as the DPPH method (or DPPH radical scavenging activity) [26]. In our study *TAC* was obtained using Eq. (3), where Abs_0 refers to the initial absorbance of the DPPH radical (at 517 nm) and $Abs_{30\min}$ the absorbance recorded at the same wavelength after 30 min.

$$TAC = \frac{Abs_0 - Abs_{30\,\min}}{Abs_0} \times 100 \quad (3)$$

As we can see in Table 1, 4-AAP has the highest value (95%), followed by compound **4** (74%) and **6** (63%); very weak antioxidant activity has been noticed for compound **1** (12%) and **5** (17%).

2.2.3. Antimicrobial evaluation

The antimicrobial activity of the investigated compounds was tested against bacterial strains isolated from clinical specimens as well as reference strains belonging to the Gram-positive (*Staphylococcus sp., Crynebacterium sp. Enterococcus faecalis*) and Gram-negative (*Escherichia coli*, *Klebsiella oxytoca*, *Klebsiella pneumonia*, *Pseudomonas aeruginosa*, *Acinetobacter baumannii*, *Serratia marcescens*, *Shigella sonnei*, *Salmonella Typhimurium*, *Stenotrophomonas maltophilia*, *Enterobacter cloacae*) species.

The qualitative screening of the susceptibility for both reference and clinical strains was performed by an adapted diffusion technique. Our results showed that the tested compounds exhibited a specific antimicrobial activity; thus, in all cases, the antimicrobial properties of the new compounds were superior to that of 4-AAP. The most active compounds have been proved to be **2**, **3** and **4** against all tested *Staphylococcus sp.* strains, *Corynebacterium sp., S. maltophilia, Acinetobacter baummanii*, and *E. faecalis* (Table 2).

In order to verify if the toxic effect is due to apoptosis, a flow cytometric assay for apoptosis that detects extracellular phosphatidylserine was carried out. 4-AAP and **1** induced few apoptosis comparing with the others; the most toxic compound is **6** (see Supplementary data for more information details).

The cell cycle commitment is slightly affected by treatment with 10 μg/mL from the compounds **1–6**: increases of G0/G1 in the case of compound **5** and **6**, or increases of G2/M phases in the case of compound **2**, **3**, and **4** were noticed. On the other hand, occurrence of apoptosis was observed in cell cycle analysis by the appearance of one peak on the left. This is due to the fact that when DNA is fragmented, as in apoptotic cells, the affinity with the intercalating PI dye is decreased and a so-called hypodiploid peak becomes apparent to the left of the G0/1 peak (see also Supplementary data).

Table 2
The antimicrobial evaluation of the new compounds **1–6** expressed as bacteria growth inhibition (+), or not (–).

Compound	**4-AAP**	**1**	**2**	**3**	**4**	**5**	**6**
Micrococcaceae							
S. aureus ATCC 25923	–	–	+	+	+	+	–
S. aureus ATCC 29213	–	–	+	+	+	+	–
S. hominis 2610	–	–	+	+	+	–	–
S. aureus 2669	–	+	+	+	+	+	–
S. aureus 2754	–	–	+	+	+	+	–
SCN 2672	–	+	+	+	+	+/–	–
SCN 3026	–	–	+	+	+	+	–
Enterobacteriaceae							
E. coli ATCC 25922	–	–	+	+	+	–	–
E. coli 410	–	–	+/–	+/–	+/–	–	–
E. coli 1455	–	–	+	+	+	–	–
E. coli 1461	–	–	–	+	–	–	–
S. typhimurium ATCC 14028	–	–	+/–	+	+/–	–	–
K. oxytoca ATCC 700324	–	–	+	+	+	–	–
K. pneumoniae 3029	–	–	–	+	–	–	–
Enterobacter cloacae 3016	–	–	–	+	–	–	–
Shigella sonnei ATCC 25931	–	–	+	+	+	–	–
Serratia marcescens 1142	–	–	–	–	–	–	–
Pseudomonadaceae							
Ps. aeruginosa ATCC 27853	–	–	+/–	+/–+	+/–	–	–
Ps. aeruginosa 1144	–	+/–	+/–	+/–	+/–	–	–
Ps. aeruginosa 1150	–	+/–	+/–	+	+/–	–	–
A. baumannii 411	–	–	+	+	+	–	–
Corynebacteriaceae							
Corynebacterium sp. 1142	–	–	+	+	+	–	–
Xanthomonadaceae							
Stenotrophomonas maltophilia 412	–	–	+	+	+	–	–
Enterococcaceae							
Enterococcus faecalis ATCC 29212	–	+/–	+	+	+	+/–	–

In conclusion, compounds **1–6** exhibit biological properties; depending on their structure, they have different antioxidant and antimicrobial activity. Compound **4**, containing twice the antipyrine moiety, has a good antioxidant and antimicrobial behavior, and a low toxicity. Further studies on these or on similar compounds may bring some new significant information.

3. Materials and methods

3.1. Apparatus and chemicals

Starting materials (chemicals, TLC plates) were achieved from Sigma–Aldrich and used as received. Solvents were purchased from Chimopar and used as received. IR spectra were recorded on a Bruker Vertex 70 spectrometer (solid sample, ATR); ^{1}H and ^{13}C NMR spectra were recorded on a Varian Inova-400 spectrometer (at selected temperatures, in deuterated solvents $CDCl_3$ and DMSO-d_6, isotopic purity 99.9%); EPR spectra were recorded on a Jeol JES-FA100 spectrometer (typical settings used for the EPR measurements: concentration of the sample 10^{-4} M, number of scans 1, centre field 3360 G, sweep field 100 G, frequency 9.42 GHz, power 1 mW, sweep time 60 s, time constant 0.1 s, modulation frequency 100 kHz, gain 100, and modulation width 1 G); UV–Vis spectra were recorded on a UVD-3500 spectrometer, in methanol at ambient temperature.

3.2. RP-TLC measurements

Chromatography was performed on 20 × 10 cm silica gel precoated plates. The plates were impregnated by overnight predevelopment in *n*-hexane-paraffin oil (95:5 v/v), then dried and kept in desiccators until used. Solutions of the compounds **1–6** were prepared in DCM and spotted on the plates. The plates were then developed in a tank chamber at room temperature using different mixtures of water and acetone (aqueous acetone solutions containing between 30% and 70% acetone). The R_f values thus obtained were used in Eqs. (1) and (2) for the determination of the lipophilicity and the hydrophobic surface area.

3.3. TAC measurements

A DPPH solution in methanol was prepared at a 2×10^{-4} M concentration. Solution of 4-AAP and compounds **1–6** were prepared also in methanol at a 0.1 mg/mL concentration. To 1.8 mL DPPH solution was added 0.2 mL solution of each compound, and the mixture kept in dark for 30 min, followed by absorbance measurement at 517 nm. The blank mixture was obtained from 1.8 mL solution of DPPH and 0.2 mL of methanol. *TAC* values were determined according to Eq. (3).

3.4. Computed Log P and PSA data

The Log *P* and *PSA* values were obtained using the Molinspiration online property calculator, based on groups contribution; the web-interactive program allows an easy calculation of molecular properties, as well as generation of data tables which may be used for structure–activity QSAR studies [25].

3.5. Antimicrobial evaluation

The qualitative screening was performed by an adapted disk diffusion method. Briefly, Petri dishes with Mueller Hinton medium were seeded with 0.5 McFarland density bacterial inocula as for the classical antibiotic susceptibility testing disk diffusion method. 5 μL of 1 mg/mL compounds were spotted on the seeded medium, at 30 mm distance. The plates were left at room temperature for 20–30 min and then incubated at 37 °C for 24 h. The positive results were read as the occurrence of an inhibition zone of microbial growth around the spot.

The eukaryotic cell culture used in our assays were represented by HCT8 (CCL-244) cells. The cells were maintained as an adherent cell line in Dulbecco's Modified Essential Medium DMEM (Sigma) supplemented with 10% foetal calf serum (Sigma) at 37 °C, 5% CO_2, in a humid atmosphere.

3.5.1. Cell viability assay

To prepare cells for plating into 96-well assay plates, adherent cells were detached, centrifuged, suspended in fresh medium, counted by tripan blue exclusion and adjusted to 5×10^4 cells/mL. Cells were dispensed into assay plates (100 μL/well) and briefly equilibrated at 37 °C, in 5% CO_2 prior to addition of the compounds **1–6**. The compounds were initially dissolved into DMSO to prepare a concentrated stock solution and additional dilutions were prepared in culture medium. Different dilutions were added to cell culture in 96-well assay plates. After 24 h, tetrazolium reduction was measured using Cell Titer 96 Aqueous One Solution Cell Proliferation assay (Promega Corporation, USA, a colorimetric method). 20 μL of CellTiter Solution were directly added to each well and plates were incubated to 37 °C, in 5% CO_2 for 1–4 h, to allow viable cells to convert tetrazolium into formazan. Plates were shaken for at least 10 min prior to determining absorbance at 490 nm. Samples were run in triplicate, and each experiment was repeated three times.

3.5.2. Apoptosis detection

In order to establish the treatment effect and to discriminate between intact and apoptotic HCT8 cells we used Annexin V-FITC Apoptosis Detection Kit I (BD Bioscience Pharmingen, USA), according to manufacturer protocol. Briefly, 5×10^5 cells were seeded in 25 cm^2 flask and treated with 100 μg/mL of the compounds **1–6** for 24 h. The total cells were resuspended in 100 μL of binding buffer (10 mM of HEPES/NaOH, pH value of 7.4, 140 mM of NaCl, and 2.5 mM of $CaCl_2$), and stained with 5 μL Annexin V-FITC and 5 μL propidium iodide for 10 min in dark. At least 10,000 events from each sample were acquired using a Beckman Coulter flow cytometer. The percentage of treatment affected cells was determined by subtracting the percentage of apoptotic/necrotic cells in the untreated population from percentage of apoptotic cells in the treated population.

3.5.3. Cell cycle distribution

5×10^5 cells were plated in 25 cm^2 flasks and treated for 40 h with 10 μg/mL from each compounds **1–6**. After treatment period cells were taken from the substrate, fixed in 70% cold ethanol for at least 30 min at −20 °C, washed twice in PBS, and then incubated 15 min, at 37 °C, with RNAse A (10 mg/mL), and 1 h with propidium iodide (10 mg/mL). After staining of cells with propidium iodide the acquisition was done using Epics Beckman Coulter flow cytometer. Data were analysed using Beckman Coulter XLM software and expressed as fractions of cells in the different cycle phases.

3.6. Synthesis

3.6.1. Compound *1*: Method 1

To 203 mg 4-AAP (1 mmol) dissolved in 50 mL DCM were added 312 mg (1 mmol) 4-carboxybenzo-15-crown-5 ether, followed by 230 mg dicyclocarbodiimide (DCC, 1.1 mmol), and the mixture left at room temperature for 3 days and filtered off. The organic phase was extracted twice with 50 mL acid aqueous hydrochloric acid (1 M), and then twice with 50 mL aqueous sodium hydrogen car-

bonate (3%), followed by 50 mL water. The organic phase was then dried on anhydrous sodium sulfate, filtered off, and the solvent removed using a rotavap. The components of the residue were separated using preparate TLC, showing only traces of the desired compound (~5%).

3.6.2. Method 2

312 mg (1 mmol) 4-carboxybenzo-15-crown-5 ether were dissolved in 25 mL dichloretane, and 0.5 mL thionyl chloride and one drop of DMF were added. The mixture was refluxed for 0.5 h, and then the solvent and the excess of thionyl chloride were removed *in vacuo* using a rotavap, yielding quantitatively the corresponding acid chloride. The acid chloride was dissolved in 25 mL DCM, and 203 mg 4-AAP (1 mmol) dissolved in 25 mL DCM were added, followed by 1 mL triethylamine. The reaction mixture was left overnight at room temperature, and the next day was extracted twice with 50 mL aqueous hydrochloric acid (1 M), and then twice with 50 mL aqueous sodium hydrogen carbonate (3%), followed by 50 mL water. The organic phase was then dried on anhydrous sodium sulfate, filtered off, and the solvent removed using a rotavap. The residue was chromatographied using a silica gel column (or preparative TLC plates) and ethyl acetate as eluent. Yields: ~50%.

Elemental analysis: $C_{26}H_{31}N_3O_7$, M = 497; calc.: C = 62.77%, H = 6.28%, N = 8.45%; found: C = 62.97%, H = 6.33%, N = 8.41%.

^{1}H NMR($CDCl_3$, δ ppm, *J* Hz): 8.87(bs, 1H, H-8); 7.56–7.21(m, 7H, H3, H-5, H-17–H-21); 6.73(bd, 1H, H-6, 8.0); 4.07(m, 4H, H-22, H-23); 3.92–3.66(m, 12H, H-CE); 3.05(s, 3H, H-15); 2.20(s, 3H, H-14).

^{13}C NMR($CDCl_3$, δ ppm): 165.93(C-7); 162.19(C-13); 151.93(C-16); 150.19(Cq); 148.48(Cq); 134.47(Cq); 129.38(C-18, C-20); 126.43(C-19); 124.80(C-17, C-21); 123.69(C-9); 121.51(C-5); 112.38(C-6); 113.02(C-3); 108.72(C-10); 71.04(CH_2—O); 70.36(CH_2—O); 69.24(CH_2—O); 68.65(CH_2—O); 35.96(C-15); 12.43(C-10).

IR(ATR in solid, ν cm^{-1}): 3454; 3272, 2925, 2870, 1645, 1591, 1494, 1452, 1297, 1266, 1213, 1128, 1048, 935, 761, 586.

UV–Vis (methanol, λ_{max} nm): 261.

R_f (silicagel, ethyl acetate): 0.08.

*3.6.3. Compound **2**: Method 1*

To 225 mg 4-AAP (1.1 mmol) dissolved in 75 mL chloroform were added 200 mg (1 mmol) 7-nitro-4-chlorobenzofurazan and 1 mL triethylamine, and the reaction mixture left overnight at room temperature. Next day the organic phase was extracted twice with 75 mL aqueous hydrochloric acid (1 M), followed twice by 75 mL aqueous sodium hydrogencarbonate (3%), and then by 75 mL water. The organic phase was then dried over anhydrous sodium sulfate, filtered off and the solvent removed under vacuo. TLC on silica gel plates and ethyl acetate as eluent showed the desired compound only in small amount (~5%) together with many other unidentified compounds.

3.6.4. Method 2

To 225 mg 4-aminoantipyrine (1.1 mmol) dissolved in 10 mL DMF were added 200 mg (1 mmol) 7-nitro-4-chlorobenzofurazan and 200 mg solid sodium hydrogencarbonate, and the mixture stirred at room temperature for 6 h. 100 mL of cold water were added to the previous mixture, and the solid formed was filtered off and dried. The residue thus obtained was purified on preparative TLC, using silica gel plates and ethyl acetate as eluent. Yields: ~20%.

Elemental analysis: $C_{17}H_{14}N_6O_4$, M = 366; calc.: C = 55.74%, H = 3.85%, N = 22.94%; found: C = 55.61%, H = 3.85%, N = 22.78%.

^{1}H NMR($CDCl_3$, δ ppm, *J* Hz): 8.92(bs, 1H, H-8 deuterable); 8.25(d, 1H, H-13, 8.6); 7.53(t, 2H, H-17, H-19, 7.6); 7.44(d, 2H, H-16, H-20, 7.6); 7.40(t, 1H, H-18, 7.6); 6.13(d, 1H, H-14, 8.6); 3.26(s, 3H, H-6); 2.21(s, 3H, H-7).

^{13}C NMR($CDCl_3$, δ ppm, T = 303 K): 161.45(C-5); 150.76(C-15); 144.17(Cq); 143.84(Cq); 143.20(Cq); 135.33(C-13); 133.94(Cq); 129.77(Cq); 128.64(C-17, C-19); 128.13(C-18); 125.40(C-16, C-20); 107.52(C-3); 101.93(C-14); 35.52(C-6); 11.03(C-3).

FT-IR(ATR in solid, ν cm^{-1}): 3463; 3175; 3115; 3051; 2925; 2856 m; 1642; 1584; 1533; 1493; 1442; 1404; 1298; 1153; 1033; 999; 906; 714.

Fluorescence (methanol, $\lambda_{max\ emission}$ nm): 440.

UV–Vis (methanol, λ_{max} nm): 324.

R_f (silicagel, ethyl acetate): 0.46.

*3.6.5. Compounds **3** and **4***

To 450 mg 4-AAP (2.2 mmoli) dissolved in 100 mL DCM were added 530 mg (2 mmoli) 4-chloro-3,5-dinitrobenzoic acid and 2 mL triethylamine, and the mixture left at room temperature. Next day the organic phase was extracted twice with 100 mL aqueous hydrochloric acid (1 M), and then twice with 100 mL aqueous sodium hydrogen carbonate (3%), followed by 100 mL water. The organic phase was then dried on anhydrous sodium sulfate, filtered off, and the solvent removed using a rotavap. The residue was chromatographied using a silica gel column (or preparative TLC plates) and ethyl acetate as eluent. Yields: **3** ~80%; **4** ~20%.

*3.6.6. Compound **3***

Elemental analysis: $C_{18}H_{14}ClN_5O_6$, M = 431.5; calc.: C = 50.07%, H = 3.27%, N = 16.22%; found: C = 50.10%, H = 3.25%, N = 16.09%.

^{1}H NMR(DMSO-D6, δ ppm, *J* Hz): 10.19(s, 1H, HN, deuterable); 8.90(s, 2H, H-10, H-14); 7.52(dd, 2H, H-17, H-19, 7.4, 8.4); 7.38(dd, 2H, H-16, H-20, 1.3, 8.4); 7.35(tt, 1H, H-18, 1.3, 7.4); 3.13(s, 3H, H-6); 2.21(s, 3H, H-3).

^{13}C NMR(DMSO-D6, δ ppm): 161.37(C-5); 161.17(C-8); 152.43(C-15); 148.75(C-11, C-13); 134.89(C-12); 129.15(C-17, C-19); 127.65(C-10, C-14); 126.55(C-18); 123.91(C-16, C-20); 121.72(C = 4); 106.16(C-3); 35.77(C-6); 11.06(C-7).

IR(ATR in solid, ν cm^{-1}): 3180, 3069, 2930, 2851, 1731, 1672, 1621, 1538, 1489, 1449, 1347, 1297, 1239, 1060, 918, 694, 586.

UV–Vis (methanol, λ_{max} nm): 277.

R_f (silicagel, ethyl acetate): 0.73.

*3.6.7. Compound **4***

Elemental analysis: $C_{29}H_{26}N_8O_7$, M = 598; calc.: C = 58.19%, H = 4.38%, N = 18.72%; found: C = 58.11%, H = 4.50%, N = 18.79%.

^{1}H NMR($CDCl_3$, δ ppm, *J* Hz): 8.70(s, 2H, H-10, H-14); 7.51–7.28(m, 10H, H-16–H-20, H-27–H-31, H-arom); 3.12(s, 3H, H-6); 3.10(3H, H-25); 2.30(s, 3H, H-7); 2.10(s, 3H, H-24).

^{13}C NMR($CDCl_3$, δ ppm, *T* = 303 K): 162.09(C-5); 161.12(C-8); 160.72(C-23); 150.73(C-15 or C-26); 150.66(C-26 or C-15); 150.18(C-11 or C-13); 149.37(C-11 or C-13); 139.51(Cq); 138.80(Cq); 134.49(C-12); 133.94(C-26); 121.84(C-4, C-21); 129.48(C-28, C-30); 129.25(C-17, C-19); 127.83(C-10, C-14); 127.37(C-29); 127.34(C-18); 125.71(C-27, C-31); 124.83(C-16, C-20); 109.16(C-22); 107.83(C-3); 35.88(C-6); 35.58(C-25); 11.78(C-24); 10.73(C-7).

FT-IR(ATR in solid, ν cm^{-1}): 3435; 3221; 2994; 2927; 1620; 1528; 1487; 1453; 1418; 1345; 1274; 1139; 1103; 1062; 1024; 921; 756; 720; 638.

UV–Vis (methanol, λ_{max} nm): 278.

R_f (silicagel, ethyl acetate): 0.09.

Compound **4** may be obtained also in good yields (80%) from **3** in reaction with 4-AAP in the presence of triethylamine, following a similar procedure.

*3.6.8. Compound **5***

To 215 mg compound **3** (0.5 mmol) dissolved in 50 mL DCM were added 120 mg (0.75 mmol) 4-aminotempo and 1 mL triethylamine, and the reaction mixture left for 3 days at room tempera-

ture. The organic phase was then extracted twice with 50 mL aqueous hydrochloric acid (1 M), and then twice with 50 mL aqueous sodium hydrogen carbonate (3%), followed by 50 mL water. The organic phase was then dried on anhydrous sodium sulfate, filtered off, and the solvent removed using a rotavap. The residue was chromatographied using a silica gel column (or preparative TLC plates) and ethyl acetate/DCM 1/1 (v/v) as eluent. Yields: ~80%.

Elemental analysis: $C_{27}H_{32}N_7O_7$, M = 566; calc.: C = 57.24%, H = 5.69%, N = 17.30%; found: C = 57.41%, H = 5.85%, N = 17.18%.

EPR (DCM, Gauss): 15.40.

IR(ATR in solid, ν cm^{-1}): 3329; 2974; 2921; 2853; 1624; 1527; 1492; 1457; 1353; 1277; 1180; 1104; 920; 693; 586; 500.

UV–Vis (methanol, λ_{max} nm): 280.

R_f (silicagel, ethyl acetate): 0.75.

3.6.9. Compound **6**

To 215 mg compound **3** (0.5 mmol) dissolved in 50 mL DCM were added 137 mg (1 mmol) isoniazid and 10 mL triethylamine. The reaction mixture was left for 3 days at room temperature, and then the organic phase was extracted twice with 50 mL aqueous hydrochloric acid (1 M), and then twice with 50 mL aqueous sodium hydrogen carbonate (3%), followed by 50 mL water. The organic phase was then dried on anhydrous sodium sulfate, filtered off, and the solvent removed using a rotavapor. The residue was chromatographied using a silica gel column (or preparative TLC plates) and DCM/methanol 9/1 (v/v) as eluent. Yields: ~60%.

Elemental analysis: $C_{24}H_{20}N_8O_7$, M = 532; calc.: C = 54.14%, H = 3.79%, N = 21.04%; found: C = 54.11%, H = 3.85%, N = 20.98%.

^{1}H NMR(DMSO-D6, δ ppm, J Hz, T = 353 K): 11.85(vbs, NH, deuterable); 9.55(s, NH, deuterable); 8.63(bs, 2H, H-10, H-14); 8.56(bd, 2H, H-24, H-25, 4.3); 7.69(d, 2H, H-23, H-26, 4.3); 7.51(t, 2H, H-17, H-19, 7.6); 7.40(d, 2H, H-16, H-20, 7.6); 7.33(t, 1H, H-18, 7.6); 3.10(s, 3H, H-6); 2.18(s, 3H, H-7).

^{13}C NMR(DMSO-D6, δ ppm): 171.88(C-21); 162.37(C-5); 161.76(C-8); 152.64(C-15); 149.40(C-24, C-25); 149.34(C-22); 144.18(Cq); 133.89(Cq); 133.55(C-4); 129.73(C-10, C-14); 129.05(C-17, C-19); 126.23(C-18); 123.58(C-16, C-20); 121.15(C-23, C-26); 116.71(Cq); 107.32(C-3); 35.92(C-6); 11.03(C-7).

FT-IR(ATR in solid, ν cm^{-1}): 3391; 3258; 3072; 2965; 2922; 2853; 1623; 1595; 1528; 1490vs; 1407; 1362; 1281; 1221; 1180; 1144; 1103; 1066; 749.

UV–Vis (methanol, λ_{max} nm): 358.

R_f (silicagel, ethyl acetate): 0.02.

Acknowledgment

This work was partially supported by a Grant of the Romanian National Authority for Scientific Research, CNCS – UEFISCDI, project number PN-II-ID-PCE-2011-3-0408.

Appendix A. Supplementary material

Supplementary data associated with this article can be found, in the online version, at doi:10.1016/j.bioorg.2011.12.003.

References

[1] D. Costa, A.P. Marques, R.L. Reis, J.L.F.C. Lima, E. Fernandes, Free Radical Biol. Med. 40 (2006) 632–640.
[2] A. Wong, WHO Pharm. Newsl. 1 (2002) 15–16.
[3] M.H.W.A. Wijnen, S.A.J. Coolen, H.L. Vader, J.C. Reijenga, F.A. Huf, R.M.H. Roumen, J. Surgical Res. 96 (2001) 183–187.
[4] E.P. Meijer, S.A.J. Coolen, A. Bast, K.R. Westerterp, Free Rad. Res. 35 (2001) 435–443.
[5] M. Danhof, D.P. Krom, D.D. Breimer, Xenobiotica 9 (1979) 695–702.
[6] M. Dandof, D.D. Breimer, Br. J. Clin. Pharm. 8 (1979) 529–537.
[7] J. Böttcher, H. Bässmann, I. Erxleben, H.M. Schiebel, J. Anal. Appl. Pyrol. 6 (1984) 1–18.
[8] S.E. Forest, M.J. Stimson, J.D. Simon, J. Phys. Chem. B103 (1999) 3963–3964.
[9] P.M.P. Santos, A.M.M. Antunes, J. Noronha, E. Fernandes, A.J.S.C. Vieira, Eur. J. Med. Chem. 45 (2010) 2258–2264.
[10] D. Costa, A. Gomes, J.L.F.C. Lima, E. Fernandes, Redox Rep. 13 (2008) 153.
[11] D. Costa, A. Vieira, E. Fernandes, Redox Rep. 11 (2006) 136–142.
[12] B. Kalyanaraman, P.G. Sohnle, J. Clin. Invest. 75 (1985) 1622.
[13] J.P. Uetrecht, H.M. Ma, E. MacKnight, R. McClelland, Chem. Res. Toxicol. 8 (1995) 226–233.
[14] N.V. Bashkatova, E.I. Korotkova, Y.A. Karbainov, A.Y. Yagovkin, A.A. Bakibaev, J. Pharm. Biomed. Anal. 37 (2005) 1143–1147.
[15] T. Rosu, E. Pahontu, C. Maxim, R. Georgescu, N. Stanica, G.L. Almajan, A. Gulea, Polyhedron 29 (2010) 757–766.
[16] T. Rosu, M. Negoiu, S. Pasculescu, E. Pahontu, D. Poirier, A. Gulea, Eur. J. Med. Chem. 45 (2010) 774–781.
[17] F. Supek, T.S. Ramljak, M. Marjanovic, M. Buljubasic, G. Kragol, N. Ilic, T. Smuc, D. Zahradka, K.M. Majerski, M. Kralj, Eur. J. Med. Chem. 46 (2011) 3444–3454.
[18] T. Orbegozo, J.G. de Vries, W. Kroutil, Eur. J. Org. Chem. 18 (2010) 3445–3448.
[19] T. Delaine, VB. Genisson, A. Quemard, P. Constant, B. Meunier, J. Bernadou, Eur. J. Med. Chem. 45 (2010) 4554–4561.
[20] T.G. Mayer, R. Weingart, F. Munstermann, T. Kawada, T. Kurzchalia, R.R. Schmidt, Eur. J. Org. Chem. 10 (1999) 2563–2571.
[21] M. Zhao, Z. Li, Y.H. Wu, Y.R. Tang, C. Wang, Z.D. Zhang, S.Q. Peng, Eur. J. Med. Chem. 42 (2007) 955–965.
[22] D. Sharma, B. Narasimhan, P. Kumar, A. Jalbout, Eur. J. Med. Chem. 44 (2009) 1119–1127.
[23] C. Hansch, A. Leo, S.B. Mekapati, A. Kurup, Bioorg. Med. Chem. 12 (2004) 3391–3400.
[24] G. Ionita, T. Constantinescu, P. Ionita, J. Planar Chromatogr. Modern TLC 11 (1998) 141–1444.
[25] http://www.molinspiration.com.
[26] R.L. Prior, X. Wu, K. Schaich, J. Agric. Food Chem. 53 (2010) 4290–4302.